J. Plasma Phys. (2018), *vol.* 84, 905840602 © Cambridge University Press 2018
doi:10.1017/S0022377818001071

Symmetric spectrum current drive due to finite radial drift effects

Peter J. Catto†

Plasma Science and Fusion Center, Massachusetts Institute of Technology, Cambridge, MA 02139, USA

(Received 17 August 2018; revised 3 October 2018; accepted 4 October 2018)

The drift surfaces of minority heated ions differ from flux surfaces due to finite poloidal gyroradius effects. As the minority poloidal gyroradius approaches radial scale lengths in the plasma, the difference between drift and flux surfaces can modify the heating and lead to a symmetric spectrum minority counter-current being driven. In response, a corresponding overall net co-current of comparable size is driven. This beneficial symmetric spectrum current drive in a tokamak is due to the parallel velocity asymmetry in the drift departure from a flux surface. As this new source of driven current is a side effect of minority heating it comes without any additional economic cost to reactor power balance. The symmetric spectrum current driven for near Maxwellian minorities is evaluated by an adjoint method and found to be modest. However, minority heating typically results in strong non-Maxwellian features on minority distributions so it may be possible to drive a significantly larger co-current. A related evaluation is performed for alpha particles in a deuterium minority heated plasma with a tritium majority. The low density of the alphas tends to keep this driven symmetric spectrum current small, but at very high heating levels a significant co-current might be driven. Other mechanisms to drive co-current with a symmetric spectrum are discussed and estimated, including asymmetric electron drag and focusing of the applied minority heating radio frequency fields.

Key words: fusion plasma, plasma flows, plasma heating

1. Introduction

Finite radial drift departures from a flux surface lead to the appearance of a 'radial' action variable or canonical angular momentum derivative in the quasilinear operator for heating and current drive as shown by Kaufman (1972) and Eriksson & Helander (1994). These 'radial' derivative terms are a direct result of the use of an action-angle set of canonical coordinates mixing configuration space and velocity space in transit averaged descriptions. The mixing of velocity and configuration space variables becomes awkward to deal with, however, when current and charge densities are formed by integrating over all velocity space for use in a full wave treatment of wave propagation that solves Maxwell's equations in configuration space (Brambilla 1999; Jaeger *et al.* 2002). In particular, when spatial derivatives arise in transit averaged quasilinear treatments due to this mixed variable behaviour (Petrov

† Email address for correspondence: catto@psfc.mit.edu

https://doi.org/10.1017/S0022377818001071 Published online by Cambridge University Press

& Harvey 2016), they must be dealt with in such a way that particle conservation is maintained so no particle sources or sinks are introduced by the heating and/or current drive in the configuration space of Maxwell's equations. This subtle behaviour is discussed for both non-transit averaged and transit averaged formulations of the quasilinear operator in tokamak geometry.

More importantly, as minority heated charges move on drift surfaces to preserve their canonical angular momentum, large poloidal gyroradius departures from flux surfaces can lead to finite orbit minority effects that may need to be retained for minority heating and current drive (Cottrell & Start 1991; Eriksson *et al.* 1998; Mantsinen *et al.* 2002). Indeed, finite orbit minority effects are thought to play a role in sawtooth control (Hellsten, Carlsson & Eriksson 1995; Chapman *et al.* 2015).

The treatment of finite orbit effects considered here takes as its starting point the quasilinear operator recently derived by Catto, Lee & Ram (2017) in tokamak geometry for heating and current drive. Some key details of this operator are briefly summarized in § 2. This non-transit averaged quasilinear operator extends the constant magnetic field result of Kennel & Engelmann (1966) to retain toroidal effects by including the magnetic drift, as well as the usual Doppler broadening of the wave–particle resonance. The detailed form is given at the start of § 3. The operator is derived by using the high frequency gyrokinetics treatment of Lee, Myra & Catto (1983) which carefully keeps the distinction between particle and guiding centre locations as in standard low frequency gyrokinetics (Catto 1978). This distinction is possible because the quasilinear derivation only requires the treatment of unperturbed trajectories so techniques developed for low frequency gyrokinetics (Catto, Tang & Baldwin 1981; Kagan & Catto 2008; Parra & Catto 2008; Parra & Calvo 2011; Calvo & Parra 2012) can be employed to higher order in the gyroradius over the unperturbed scale length expansion to remove gyrophase dependent terms in the Vlasov operator as in Lee *et al.* (1983).

The quasilinear derivation of Catto *et al.* (2017) does not explicitly claim to retain finite orbit drift effects. However, because they keep the distinction between particle and guiding centre locations, the non-transit averaged form they derive is able to treat the drift off of a flux surface as charges drift radially to preserve their canonical angular momentum. This feature means that motion of a charge through a wave–particle resonance need only be adapted to account for the fact that the drifting charge moves in a manner that conserves its canonical angular momentum. This adjustment automatically preserves the negative definite entropy production property of their quasilinear operator while preserving the distinction between drift and flux surfaces. These features are discussed in detail in the remainder of § 3.

To explicitly evaluate finite orbit effects the quasilinear operator is transit averaged along the actual charged particle trajectory that preserves its canonical angular momentum as it passes through resonance. This procedure introduces a finite drift correction to the transit average quasilinear diffusivity as discussed in § 4. This finite drift departure term allows the minority current to be driven with a symmetric heating spectrum by a mechanism different than the neoclassical streaming effect considered by Helander & Catto (2001) for electron cyclotron heating in a tokamak. The new mechanism arises because the finite orbit departure from a flux surface is asymmetric in the parallel velocity $v_{||}$ along the magnetic field such that the counter-current direction of $v_{||}$ charges are heated more than the co-current directed ones. As shown in figure 1, the heating difference between the counter and co-moving ions occurs because the counter (co) have a longer (shorter) interaction time with the applied radio frequency (rf) as discussed in §§ 4 and 5. As an example, the current driven by

https://doi.org/10.1017/S0022377818001071 Published online by Cambridge University Press

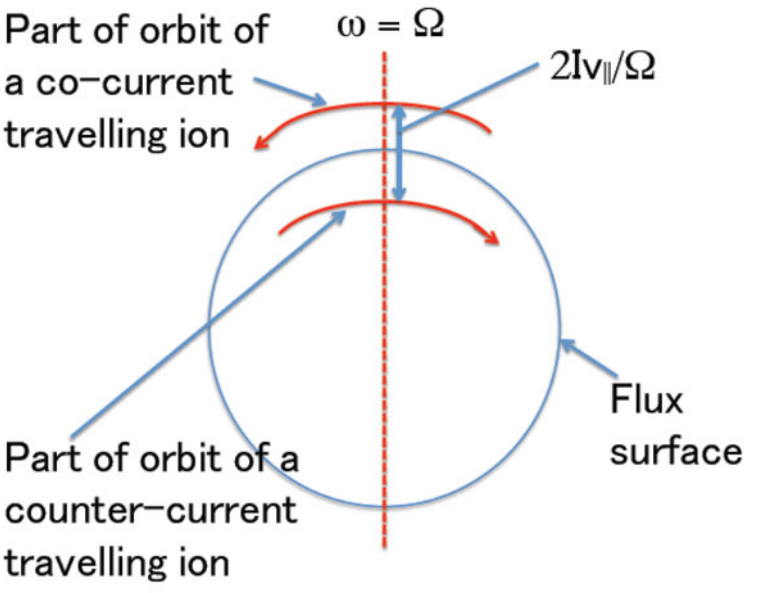


FIGURE 1. More (less) minority heating always occurs in the counter (co) current direction because the interaction time $\tau_{\rm int} \propto q/\varepsilon$ for the counter (co) travelling minorities that are closer to (further from) the magnetic axis is longer (shorter) as shown here schematically. Therefore, excess minority heating always occurs in the favourable counter-current direction.

a symmetric spectrum is evaluated for a near Maxwellian minority species in § 5. In this limit the driven current is found to be rather modest so is unlikely to be useful. However, minority heating levels are often large enough to result in substantial departures from a Maxwellian. Therefore, it may be possible to drive significant minority counter-current with a symmetric spectrum, and thereby generate beneficial driven co-current. Detailed simulations seem necessary to make this determination. These could even be performed for deuterium and energetic alpha minorities in a tritium plasma.

Once we evaluate the parallel flow of the energetic minorities, $V_{||m}$, for a symmetric spectrum it is important to ascertain the direction of the overall parallel current that is driven to determine if it is in the desirable co-current direction or the unfavourable counter-current direction. To make this determination we follow the insights outlined by Fisch (1981) for a conventional minority current drive that relies on an asymmetry in the collisional heating. When there is no net parallel momentum input we assume we must satisfy

$$Mn_m V_{||m} + mn_e V_{||e} + M_i n_i V_{||i} = 0 \tag{1.1}$$

in our quasineutral plasma with

$$Zn_m + Z_i n_i = n_e. \tag{1.2}$$

We use n, $V_{||}$, Z and M to signify density, parallel fluid velocity, charge number and mass, with the subscripts i, e and m denoting background ion, electron and minority

https://doi.org/10.1017/S0022377818001071 Published online by Cambridge University Press

species, with m the electron mass and $Z=-1$ the electron charge. The m subscript is suppressed on the minority charge number Z and mass M. The friction between the electrons, and minorities and background ions must vanish (Fisch 1981) to lowest order to satisfy the parallel electron momentum equation giving

$$Z^2 n_m (V_{||m} - V_{||e}) + Z_i^2 n_i (V_{||i} - V_{||e}) = 0. \tag{1.3}$$

This friction equation is more carefully obtained by multiplying the parallel electron momentum equation by the magnetic field B and then flux surface averaging to annihilate the electron pressure and the electrostatic potential term (assuming Maxwell–Boltzmann responses to lowest order). As we are not concerned about inverse aspect ratio corrections, the procedure of Fisch (1981) is adequate for our purposes.

These three equations determine the direction of the parallel current

$$J_{||} = Z e n_m V_{||m} + Z_i e n_i V_{||i} - n_e e V_{||e} \tag{1.4}$$

once the direction of $V_{||m}$ is known, as can be seen by neglecting the parallel momentum of the electrons as small to find

$$M_i n_i V_{||i} = -M n_m V_{||m}, \tag{1.5}$$

and then using the vanishing of the electron friction to obtain

$$V_{||e} = \frac{Z^2 n_m V_{||m} + n_i V_{||i}}{Z^2 n_m + Z_i^2 n_i} = \frac{(Z^2 - Z_i^2 M/M_i) n_m V_{||m}}{Z^2 n_m + Z_i^2 n_i}. \tag{1.6}$$

From these expressions we can already see that a negative parallel minority flow ($V_{||m} < 0$), results in a positive parallel main ion flow ($V_{||i} > 0$) and a negative parallel electron flow ($V_{||e} < 0$), thereby resulting in the possibility of co-current being driven. Eliminating $V_{||e}$ and $V_{||i}$ the symmetric spectrum co-current can be written as

$$J_{||} = -Z e n_m V_{||m} \frac{Z_i (Z - Z_i)(n_i - M n_m/M_i)}{Z_i^2 n_i + Z^2 n_m}, \tag{1.7}$$

which for $V_{||m} < 0$ and $Z > Z_i$ will be co-current as long as $n_i > M n_m/M_i$. In the subsequent sections we will demonstrate that when finite poloidal gyroradius effects are retained, a counter-current minority flow is ordinarily driven. Therefore, when a minority species is present a symmetric heating spectrum will normally result in co-current drive.

We also consider a second example of minority deuterium (D) heating in a tritium (T) plasma in § 6. In this case the amount of alpha counter-current driven tends to remain small as the alpha density is much smaller than the plasma density. However, at high minority heating levels it may be possible to drive modest and perhaps even significant co-current. The closing section summarizes results, but also discusses other possible ways to drive co-current with a symmetric spectrum.

https://doi.org/10.1017/S0022377818001071 Published online by Cambridge University Press

2. Formulation of the quasilinear equation

We start with full Fokker–Planck kinetic equation

$$\partial f/\partial t + \boldsymbol{v}\cdot\nabla f + (Ze/M)[\boldsymbol{e} + c^{-1}\boldsymbol{v}\times(\boldsymbol{B}+\boldsymbol{b})]\cdot\nabla_u f = C\{f\}, \tag{2.1}$$

with $\boldsymbol{e} = \boldsymbol{e}(\boldsymbol{r}, t)$ and $\boldsymbol{b} = \boldsymbol{b}(\boldsymbol{r}, t)$ the applied radio frequency (rf) wave fields satisfying Faraday's law, and $\boldsymbol{B}$ the unperturbed, axisymmetric magnetic field

$$\boldsymbol{B} = B\boldsymbol{n} = I(\psi)\nabla\zeta + \nabla\zeta\times\nabla\psi. \tag{2.2}$$

Here ζ is the toroidal angle variable and $I = RB_t$ is a function of the poloidal flux function ψ, with B_t and B_p the toroidal and poloidal magnetic fields. We denote $\boldsymbol{e}_1$ as the unit vector in the $\nabla\psi$ direction by taking $\nabla\psi = RB_p\boldsymbol{e}_1$, and let $\boldsymbol{e}_2 = \boldsymbol{n}\times\boldsymbol{e}_1$ be the orthonormal unit vector. The notation is as in Catto *et al.* (2017).

Our quasilinear treatment begins in what appears to be the usual manner by taking

$$f = f_0 + f_1 + \cdots, \tag{2.3}$$

with $f_1 \ll f_0$. However, the unperturbed drift kinetic operator acting on the unperturbed distribution function f_0 must vanish for the gyrophase independent drift kinetic canonical angular momentum, as recalled in (2.8) below. The full gyrophase dependent canonical angular momentum ψ_* is

$$\psi_* \equiv \psi - (Mc/Ze)R^2\nabla\zeta\cdot\boldsymbol{v} \equiv \bar{\psi}_* + \Omega^{-1}\boldsymbol{v}\times\boldsymbol{n}\cdot\nabla\psi, \tag{2.4}$$

where the drift kinetic form $\bar{\psi}_*$ written in terms of ψ, ϑ, v, μ, and σ is

$$\bar{\psi}_* \equiv \psi - Iv_{||}/\Omega = \psi - \Omega^{-1}I\sigma\sqrt{v^2 - 2\mu_0 B} = \psi - \Omega^{-1}Iv\sigma\sqrt{1-\lambda B/B_0}, \tag{2.5}$$

with $\Omega = ZeB/Mc$, $\mu_0 = v_\perp^2/2B(\boldsymbol{r})$ the lowest order magnetic moment, $\sigma = v_{||}/|v_{||}|$ the sign of $v_{||} = \boldsymbol{n}\cdot\boldsymbol{v} = \sigma\sqrt{v^2 - 2\mu_0 B}$, v the speed $v = |\boldsymbol{v}| = \sqrt{v_\perp^2 + v_{||}^2}$, $\lambda = 2\mu_0 B_0/v^2$, ϑ the poloidal angle, φ the gyrophase, and

$$\boldsymbol{v} = \boldsymbol{v}_\perp + v_{||}\boldsymbol{n} = v_\perp[\boldsymbol{e}_1(\boldsymbol{r})\cos\varphi + \boldsymbol{e}_2(\boldsymbol{r})\sin\varphi] + v_{||}\boldsymbol{n}(\boldsymbol{r}). \tag{2.6}$$

The normalizing magnetic field is $B_0 = \sqrt{\langle B^2\rangle}$ with $\langle\cdots\rangle$ a flux surface average. The last term in (2.4) is the difference between the guiding centre and particle locations, while the $Iv_{||}/\Omega$ term in (2.5) keeps the distinction between the flux and drift surfaces.

A drift kinetic treatment for f_0 can depend on the drift kinetic constant of the motion $\bar{\psi}_*$ that we treat as a dependent variable. Hence, we allow

$$f_0 = f_0(\bar{\psi}_*;\, \psi, \vartheta, v, \mu, \sigma, t), \tag{2.7}$$

with ψ, ϑ, v, μ, σ and t the same independent drift kinetic variables as in Catto *et al.* (2017), most of whose results we will be able to adopt.

The notation in (2.7) is intended to indicate that $\bar{\psi}_*$ is a dependent variable and ψ is an independent variable, thereby allowing us to distinguish between finite orbit effects and flux surface variation. The notation will allow us to explicitly display the velocity dependent finite departure of a drift surface from a flux surface.

https://doi.org/10.1017/S0022377818001071 Published online by Cambridge University Press

The drift kinetic canonical angular momentum $\bar{\psi}_*$ is convenient to employ because it is a drift kinetic constant of the motion satisfying

$$(v_{||}\boldsymbol{n}+\boldsymbol{v}_d)\cdot\boldsymbol{\nabla}\bar{\psi}_*=-\boldsymbol{v}_d\cdot\boldsymbol{\nabla}(Iv_{||}/\Omega)=0, \tag{2.8}$$

(as shown in appendix B of Parra & Catto (2010)) where we also use $\boldsymbol{v}_d\cdot\boldsymbol{\nabla}\psi = v_{||}\boldsymbol{n}\cdot\boldsymbol{\nabla}(Iv_{||}/\Omega)$. Here we denote $\boldsymbol{v}_d$ as the magnetic drift,

$$\boldsymbol{v}_d=\Omega^{-1}\boldsymbol{n}\times(\mu\boldsymbol{\nabla}B+v_{||}^2\boldsymbol{n}\cdot\boldsymbol{\nabla}\boldsymbol{n})=\Omega^{-1}v_{||}\boldsymbol{\nabla}\times(v_{||}\boldsymbol{n}). \tag{2.9}$$

By using total energy $E=v^2/2+Ze\Phi(\psi)/M$ instead of v, as we could generalize to retain the $\boldsymbol{E}\times\boldsymbol{B}$ drift as well. To retain drift effects in the quasilinear operator we must allow f_0 to depend on the magnetic moment to higher order as shown by Catto *et al.* (2017). Therefore, we use $\mu=\mu_0+\mu_1$, where Catto *et al.* (2017) prove that only $\mu_1\to -B^{-1}\boldsymbol{v}_\perp\cdot\boldsymbol{v}_d$ and $B\boldsymbol{\nabla}_v\mu\to\boldsymbol{v}_\perp-\boldsymbol{v}_d$ need be retained.

When parallel streaming and finite orbit effects compete and dominate the lowest order drift kinetic equation is

$$(v_{||}\boldsymbol{n}+\boldsymbol{v}_d)\cdot\boldsymbol{\nabla}\bar{f}_0=0, \tag{2.10}$$

with $f_0=\bar{f}_0+\tilde{f}_0$, $\bar{f}_0\gg\tilde{f}_0$, and

$$\bar{f}_0=\bar{f}_0(\bar{\psi}_*,\,v,\,\mu,\,\sigma), \tag{2.11}$$

indicating that the ψ and ϑ dependence can only enter through $\bar{\psi}_*$.

When streaming does not dominate, the introduction of $\bar{\psi}_*$ is of no benefit. Then f_0 satisfies the quasilinear (QL) equation

$$\partial f_0/\partial t+(v_{||}\boldsymbol{n}+\boldsymbol{v}_d)\cdot\boldsymbol{\nabla}f_0+\langle\boldsymbol{a}\cdot\boldsymbol{\nabla}_v f_1\rangle_{cg,\varphi}=\langle C\{f_0\}\rangle_\varphi, \tag{2.12}$$

with the perturbed acceleration defined as

$$\boldsymbol{a}=(Ze/M)(\boldsymbol{e}+c^{-1}\boldsymbol{v}\times\boldsymbol{b}), \tag{2.13}$$

and the gyroaverages $\langle\cdots\rangle_\varphi$ performed at fixed ψ, ϑ, v, μ, σ, and t,

$$\langle\cdots\rangle_\varphi=(2\pi)^{-1}\oint\mathrm{d}\varphi(\cdots). \tag{2.14}$$

Quasilinear theory assumes that f_0 does not contain any fast time or space variation and that collisions and quasilinear diffusion compete. As a result, we take f_0 to be the coarse grain average of f,

$$f_0=\langle f\rangle_{cg}=\frac{1}{2T}\int_{t-T}^{t+T}\mathrm{d}\tau\,\frac{1}{2\Delta}\int_{\psi-\Delta}^{\psi+\Delta}\mathrm{d}\psi'\oint\frac{\mathrm{d}\zeta}{2\pi}\langle f\rangle_\vartheta, \tag{2.15}$$

where the integral over toroidal angle ζ insures axisymmetry, and the average $\langle\cdots\rangle_\vartheta$ over poloidal angle ϑ removes the exponential poloidal mode number variation. We must allow $Q\{f_0\}$ to be a slow function of ϑ in a tokamak so $\langle\cdots\rangle_\vartheta\neq(2\pi)^{-1}\oint\mathrm{d}\vartheta(\cdots)$. The integral over τ removes fast time variation by taking $\omega^{-1}\ll T\ll\nu^{-1}$, where ν and ω are the collision frequency and typical rf wave frequency, respectively. The limits on the poloidal flux function ψ integral resolve poloidal gyroradius scales by assuming

https://doi.org/10.1017/S0022377818001071 Published online by Cambridge University Press

$\Delta \ll \rho_p$, where $\rho_p = \rho B/B_p$ is the poloidal gyroradius, with ρ the species gyroradius. The radial and $\langle \cdots \rangle_\vartheta$ averages are defined so that the entropy production is negative definite, with f_0 allowed to be a slow function of ψ and ϑ.

We define the quasilinear operator Q by

$$Q\{f_0\} = -\langle \nabla_v \cdot (\boldsymbol{a} f_1) \rangle_{cg,\varphi} = -\nabla_v \cdot \langle \boldsymbol{a} f_1 \rangle_{cg,\varphi}, \tag{2.16}$$

where the drift kinetic treatment in ψ, ϑ, v, μ, σ, and t variables requires that we average the QL term over gyrophase, as well as perform a coarse grain average. The drift kinetic equation then becomes

$$\partial f_0/\partial t + (v_{||}\boldsymbol{n} + \boldsymbol{v}_d) \cdot \nabla f_0 = C\{f_0\} + Q\{f_0\}. \tag{2.17}$$

Rotational invariance allows us to use $\langle C\{f_0\} \rangle_\varphi = C\{f_0\}$ as there is no preferred direction associated with the collision operator.

The preceding equation implicitly allows us to retain $\bar{\psi}_*$ as a dependent variable when the streaming combination of (2.10) dominates due to finite orbit effects such that to lowest order $f_0 \to \bar{f}_0(\bar{\psi}_*, v, \mu, \sigma)$. Equation (2.17) is the same as Catto *et al.* (2017) since it only differs by the introduction of a dependent variable $\bar{\psi}_*$ to track finite orbit affects. That is, we now write $f_0 = f_0(\bar{\psi}_*; \psi, \vartheta, v, \mu, \sigma, t)$, rather than using $f_0 = f_0(\psi, \vartheta, v, \mu, \sigma, t)$ – a form that does not allow us to explicitly display $\bar{\psi}_*$ or 'radial' spatial derivatives of f_0 when the velocity space gradient is performed.

Here we also emphasize that our result for the quasilinear operator must have the property that it does not act as a source or sink of particles since

$$\int \mathrm{d}^3 v Q\{f_0\} = -\int \mathrm{d}^3 v \nabla_v \cdot \langle \boldsymbol{a} f_1 \rangle_{cg} = 0. \tag{2.18}$$

That is, in drift kinetic variables, there can be no diffusive spatial particle transport (or source or sink of particles) due to the operator $Q\{f_0\}$. Such a statement might appear to contradict the results of Kaufman (1972) and Eriksson & Helander (1994), but their treatments are in canonical variables that mix configuration and velocity space and thereby only appear to introduce a radial spatial derivative as we will demonstrate in § 3.

We allow both spatial heat and parallel momentum diffusive transport since

$$\int \mathrm{d}^3 v v^2 Q\{f_0\} = 2(Ze/M) \left\langle \boldsymbol{e} \cdot \int \mathrm{d}^3 v \boldsymbol{v} f_1 \right\rangle_{cg} \neq 0 \tag{2.19}$$

and

$$\int \mathrm{d}^3 v \boldsymbol{v} Q\{f_0\} = \int \mathrm{d}^3 v \langle \boldsymbol{a} f_1 \rangle_{cg} \neq 0. \tag{2.20}$$

Our choice of independent variables means we can simply adopt the quasilinear operator obtained by Catto *et al.* (2017) to illustrate how finite orbit effects enter.

https://doi.org/10.1017/S0022377818001071 Published online by Cambridge University Press

3. Quasilinear operator

Catto *et al.* (2017) derive the following self-adjoint form for the QL operator:

$$Q\{f_0\} = \sum_{\omega,p} \frac{v_{||}}{v}\left(\frac{\partial}{\partial v} + \frac{p\Omega v}{\omega B}\frac{\partial}{\partial \mu_0}\right)\left[D\frac{v}{v_{||}}\left(\frac{\partial f_0}{\partial v} + \frac{p\Omega v}{\omega B}\frac{\partial f_0}{\partial \mu_0}\right)\right], \tag{3.1}$$

with $p\Omega = \omega - k_{||}v_{||} - \boldsymbol{k}\cdot\boldsymbol{v}_d$, and

$$D = \frac{\pi Z^2 e^2}{2M^2 v^2}\sum_{\kappa,m,n}\delta(\omega - p\Omega - k_{||}v_{||} - \boldsymbol{k}\cdot\boldsymbol{v}_d)|\boldsymbol{e}_m\cdot[\boldsymbol{n}v_{||}J_p(w) + \boldsymbol{e}_{\perp p}v_\perp]|^2, \tag{3.2}$$

manifestly positive, with no quasilinear particle diffusion as required by (2.18). In this final form the entropy production is negative definite, and it is no longer necessary to keep the distinction between μ and μ_0, so we may now use $d^3v \to 2\pi vB\,\mathrm{d}v\,\mathrm{d}\mu_0/v_{||}$. To obtain this form the applied fluctuating electric field $\boldsymbol{e} = \boldsymbol{e}(\boldsymbol{r}, t)$ is Fourier decomposed poloidally (m) and toroidally (n), permitted to have more than a single applied wave frequency by Fourier decomposing in time, and allowed to possess local fine scale radial eikonal variation with multiple roots (sum over κ) due to mode conversion. Therefore, we take

$$\boldsymbol{e} = \boldsymbol{e}(\boldsymbol{r}, t) = \sum_{m,n,\omega,\kappa}\boldsymbol{e}_m \mathrm{e}^{-\mathrm{i}\omega t - \mathrm{i}n\zeta + \mathrm{i}S(\psi) + \mathrm{i}m\vartheta}, \tag{3.3}$$

with $w \equiv k_\perp v_\perp/\Omega$ the argument of the Bessel functions,

$$\boldsymbol{\kappa} = \nabla S = \nabla\psi\,\partial S/\partial\psi = \boldsymbol{e}_1 RB_p\partial S/\partial\psi = \kappa\boldsymbol{e}_1, \tag{3.4}$$

$$k_{||} = (m - qn)I/qR^2B \sim (m - qn)/qR, \tag{3.5}$$

$$\boldsymbol{k} = \boldsymbol{\kappa} + m\nabla\vartheta - n\nabla\zeta, \tag{3.6}$$

$$\boldsymbol{e}_{\perp p} = \frac{1}{2}[\boldsymbol{e}_-\mathrm{e}^{\mathrm{i}\alpha}J_{p+1}(w) + \boldsymbol{e}_+\mathrm{e}^{-\mathrm{i}\alpha}J_{p-1}(w)] = \frac{p}{k_\perp w}J_p(w)\boldsymbol{k}_\perp + \frac{\mathrm{i}}{k_\perp}J_p'(w)\boldsymbol{n}\times\boldsymbol{k}, \tag{3.7}$$

$$\boldsymbol{k}_\perp = (k_\perp/2)(\boldsymbol{e}_-\mathrm{e}^{\mathrm{i}\alpha} + \boldsymbol{e}_+\mathrm{e}^{-\mathrm{i}\alpha}), \tag{3.8}$$

and

$$\boldsymbol{e}_\pm = \boldsymbol{e}_1 \pm \mathrm{i}\boldsymbol{e}_2, \tag{3.9}$$

where $\boldsymbol{e}_+$ is the left-hand polarized wave direction of minority heating and current drive. Preserving the desired entropy production property requires

$$\langle\boldsymbol{e}\boldsymbol{e}\rangle_{cg} = \frac{1}{4}\sum_{\omega,m,n\cdot\kappa}(\boldsymbol{e}_m\boldsymbol{e}_m^* + \boldsymbol{e}_m^*\boldsymbol{e}_m). \tag{3.10}$$

Equations (3.1) and (3.2) are the results of Catto *et al.* (2017). They reduce to the QL operator of Kennel & Engelmann (1966) in a constant magnetic field. Our QL ordering like theirs allows $Q \sim C$ or $D/v_{\mathrm{tail}}^2 \sim \nu$, with $D \sim Z^2e^2|\boldsymbol{e}_m|^2/M^2\omega \sim \omega v_{\mathrm{quiv}}^2$ and $v_{\mathrm{quiv}} \sim Ze|\boldsymbol{e}_m|/M\omega$. It requires small quiver speeds v_{quiv} compared to the typical minority ion tail speed v_{tail} to satisfy $v_{\mathrm{quiv}}^2/v_{\mathrm{tail}}^2 \sim \nu/\omega \ll 1$.

https://doi.org/10.1017/S0022377818001071 Published online by Cambridge University Press

To display finite orbit effects we can employ the dependent variable $\bar{\psi}_*$ to write

$$\frac{\partial}{\partial v} = \frac{\partial}{\partial v}\bigg|_{\bar{\psi}_*} + \frac{\partial \bar{\psi}_*}{\partial v}\bigg|_{\mu_0} \frac{\partial}{\partial \bar{\psi}_*} = \frac{\partial}{\partial v}\bigg|_{\bar{\psi}_*} - \frac{Iv}{\Omega v_{||}} \frac{\partial}{\partial \bar{\psi}_*} \tag{3.11}$$

and

$$\frac{\partial}{\partial \mu_0} = \frac{\partial}{\partial \mu_0}\bigg|_{\bar{\psi}_*} + \frac{\partial \bar{\psi}_*}{\partial \mu_0}\bigg|_{v} \frac{\partial}{\partial \bar{\psi}_*} = \frac{\partial}{\partial \mu_0}\bigg|_{\bar{\psi}_*} + \frac{IB}{\Omega v_{||}} \frac{\partial}{\partial \bar{\psi}_*}. \tag{3.12}$$

In this notation (3.1) gives an alternate, but not particularly useful, form displaying the effect of finite orbits by the appearance of derivatives with respect to $\bar{\psi}_*$:

$$Q\{f_0\} = \sum_{\omega,p} \frac{v_{||}}{v} \left[\frac{\partial}{\partial v}\bigg|_{\bar{\psi}_*} + \frac{p\Omega v}{\omega B} \frac{\partial}{\partial \mu_0}\bigg|_{\bar{\psi}_*} - \left(1 - \frac{p\Omega}{\omega}\right) \frac{Iv}{\Omega v_{||}} \frac{\partial}{\partial \bar{\psi}_*} \right] \times \left\{ D \frac{v}{v_{||}} \left[\frac{\partial f_0}{\partial v}\bigg|_{\bar{\psi}_*} + \frac{p\Omega v}{\omega B} \frac{\partial f_0}{\partial \mu_0}\bigg|_{\bar{\psi}_*} - \left(1 - \frac{p\Omega}{\omega}\right) \frac{Iv}{\Omega v_{||}} \frac{\partial f_0}{\partial \bar{\psi}_*} \right] \right\}. \tag{3.13}$$

If the $\bar{\psi}_*$ dependence of D is clear in (3.13), as it is when (2.10) and (2.11) hold, then the Catto *et al.* (2017) form is general enough to retain finite orbit effects with

$$(\rho_p I/\Omega \bar{f}_0)\partial \bar{f}_0/\partial \bar{\psi}_* \sim \rho_p/a_* \sim 1, \tag{3.14}$$

as well as drift effects with

$$k_{||} v_{||}/\boldsymbol{k}\cdot\boldsymbol{v}_d \sim k_{||} R/k_\perp \rho_p \sim 1. \tag{3.15}$$

Both finite orbit width and drift effects can be significant for energetic ions with a radial scale length of a_* for $\bar{f}_0$, where $\rho_p = \rho B/B_p$ denotes the energetic ion poloidal gyroradius and B_p the poloidal magnetic field.

Unlike the Hamiltonian action-angle treatments of Kaufman (1972) and Eriksson & Helander (1994), expression (3.13) for the quasilinear operator is not yet bounce or transit averaged. However, like these action-angle treatments, (3.13) makes use of a mixed velocity and configuration space variable – here the dependent mixed variable $\bar{\psi}_*$. In these mixed variables the vanishing of the particle sink or source necessary to satisfy (2.18) is not as obvious as it is in form (3.1) or its cylindrical velocity space equivalent.

4. Transit averaged quasilinear operator

When streaming dominates with finite orbit effects retained the lowest order steady state equation for f_0 requires (2.10) be satisfied with

$$f_0 = \bar{f}_0(\bar{\psi}_*, v, \mu_0, \sigma) + \tilde{f}_0(\bar{\psi}_*, \vartheta, v, \mu_0, \sigma), \tag{4.1}$$

where $\bar{f}_0 \gg \tilde{f}_0$. Then to next order we obtain

$$(v_{||}\boldsymbol{n} + \boldsymbol{v}_d)\cdot\nabla \tilde{f}_0 = C\{\bar{f}_0\} + Q\{\bar{f}_0\}. \tag{4.2}$$

https://doi.org/10.1017/S0022377818001071 Published online by Cambridge University Press

To keep finite orbit effects it is convenient to use $\bar{\psi}_*$ and ϑ as variables as the transit average must be performed along the actual drift orbit traced out at fixed $\bar{\psi}_*$. Then

$$(v_{||}\boldsymbol{n}+\boldsymbol{v}_d)\cdot\nabla\vartheta\,\partial\tilde{f}_0/\partial\vartheta|_{\bar{\psi}_*}=C\{\bar{f}_0\}+Q\{\bar{f}_0\}. \tag{4.3}$$

Ignoring ρ_p/R corrections allows us to use

$$(v_{||}\boldsymbol{n}+\boldsymbol{v}_d)\cdot\nabla\vartheta=[v_{||}-v_{||}\partial(Iv_{||}/\Omega)/\partial\psi]\boldsymbol{n}\cdot\nabla\vartheta\simeq v_{||}\boldsymbol{n}\cdot\nabla\vartheta, \tag{4.4}$$

giving

$$v_{||}\boldsymbol{n}\cdot\nabla\vartheta\,\partial\tilde{f}_0/\partial\vartheta|_{\bar{\psi}_*}=C\{\bar{f}_0\}+Q\{\bar{f}_0\}, \tag{4.5}$$

with all the poloidal gyroradius variation of interest located in $\bar{f}_0=\bar{f}_0(\bar{\psi}_*,\,v,\,\mu_0,\,\sigma)$ since we will next annihilate the $\tilde{f}_0$ term. Approximation (4.4) is consistent with integrating along an orbit of fixed $\bar{\psi}_*\equiv\psi-Iv_{||}/\Omega$ since it gives

$$\frac{\mathrm{d}\psi}{\mathrm{d}\vartheta}=\frac{\boldsymbol{v}_d\cdot\nabla\psi}{(v_{||}\boldsymbol{n}+\boldsymbol{v}_d)\cdot\nabla\vartheta}=\frac{\partial(Iv_{||}/\Omega)/\partial\vartheta}{1-\partial(Iv_{||}/\Omega)/\partial\psi}\simeq\frac{\partial(Iv_{||}/\Omega)}{\partial\vartheta}. \tag{4.6}$$

We then introduce the transit average

$$\overline{(\cdots)}=\left[\oint\mathrm{d}\vartheta(\cdots)/v_{||}\boldsymbol{n}\cdot\nabla\vartheta\right]\Big/\left[\oint\mathrm{d}\vartheta/v_{||}\boldsymbol{n}\cdot\nabla\vartheta\right], \tag{4.7}$$

where ϑ integration in the numerator and denominator is over a full poloidal circuit following a minority ion moving with fixed $\bar{\psi}_*$. For trapped ions, $v_{||}$ and ϑ change sign simultaneously at a turning point. Transit averaging the kinetic equation gives

$$\overline{C\{\bar{f}_0\}}+\overline{Q\{\bar{f}_0\}}=0, \tag{4.8}$$

where the transit averaged quasilinear operator is

$$\overline{Q\{f_0\}}=\frac{1}{v\left(\oint\mathrm{d}\tau\right)}\sum_{\omega,p}\left(\frac{\partial}{\partial v}+\frac{p\Omega v}{\omega B}\frac{\partial}{\partial\mu_0}\right)\left[v\bar{D}\left(\oint\mathrm{d}\tau\right)\left(\frac{\partial\bar{f}_0}{\partial v}+\frac{p\Omega v}{\omega B}\frac{\partial\bar{f}_0}{\partial\mu_0}\right)\right], \tag{4.9}$$

with $\bar{D}$ the transit average of the full QL diffusivity

$$\bar{D}=\bar{D}(\bar{\psi}_*,\,v,\,\mu_0,\,\sigma)=\left[\oint\mathrm{d}\vartheta D/v_{||}\boldsymbol{n}\cdot\nabla\vartheta\right]\Big/\left[\oint\mathrm{d}\vartheta/v_{||}\boldsymbol{n}\cdot\nabla\vartheta\right] \tag{4.10}$$

and $\mathrm{d}\tau=\mathrm{d}\vartheta/v_{||}\boldsymbol{n}\cdot\nabla\vartheta$. The quasilinear diffusivity $\bar{D}$ has spatial variation only via $\bar{\psi}_*$ as the transit average retains the distinction between the *rf* fields along drift and flux surfaces. A key place where finite poloidal minority gyroradius effects enter (3.2) is in the gyrofrequency Ω in the delta function. There we must Taylor expand about $\bar{\psi}_*$ using

$$\Omega=\Omega(\psi,\,\vartheta)=\Omega(\bar{\psi}_*,\,\vartheta)+(\psi-\bar{\psi}_*)\partial\Omega/\partial\psi+\cdots=\Omega_*+I\Omega^{-1}v_{||}\partial\Omega/\partial\psi+\cdots, \tag{4.11}$$

https://doi.org/10.1017/S0022377818001071 Published online by Cambridge University Press

where $\Omega_* = \Omega(\bar{\psi}_*, \vartheta)$. The correction term is small compared to Ω so the distinction between $\bar{\psi}_*$ and ψ does not matter in it. However, this small term need not be small compared to $k_{||}v_{||}$ and $\boldsymbol{k}\cdot\boldsymbol{v}_d$, so it must be retained in

$$\delta(\omega - p\Omega - k_{||}v_{||} - \boldsymbol{k}\cdot\boldsymbol{v}_d) \simeq \delta(\omega - p\Omega_* - pI\Omega^{-1}v_{||}\partial\Omega/\partial\psi - k_{||}v_{||} - \boldsymbol{k}\cdot\boldsymbol{v}_d). \quad (4.12)$$

In addition, the $\bar{\psi}_*$ and ψ distinction may need to be retained in $|\boldsymbol{e}_m \cdot [\boldsymbol{n}v_{||}J_p(w) + \boldsymbol{e}_{\perp p}v_\perp]|^2$. For now we assume this quantity varies slowly compared to a poloidal gyroradius. Consequently, we write

$$D = \frac{\pi Z^2 e^2}{2M^2 v^2} \sum_{\kappa,m,n} \delta(\omega - p\Omega_* - pI\Omega^{-1}v_{||}\partial\Omega/\partial\psi - k_{||}v_{||} - \boldsymbol{k}\cdot\boldsymbol{v}_d) \times |\boldsymbol{e}_m \cdot [\boldsymbol{n}v_{||}J_p(w) + \boldsymbol{e}_{\perp p}v_\perp]|_*^2, \quad (4.13)$$

where the subscript * indicates a quantity is to be evaluated at $\bar{\psi}_*$ (and not ψ) as it passes through the resonance where the argument of the delta function vanishes. That is, for each pass through cyclotron resonance (at $\omega \simeq p\Omega_*$ for $p \neq 0$),

$$\oint \mathrm{d}\tau \delta(\omega - p\Omega - k_{||}v_{||} - \boldsymbol{k}\cdot\boldsymbol{v}_d)|\boldsymbol{e}_m \cdot [\boldsymbol{n}v_{||}J_p(w) + \boldsymbol{e}_{\perp p}v_\perp]|^2 \rightarrow \frac{|\boldsymbol{e}_m \cdot [\boldsymbol{n}v_{||}J_p(w) + \boldsymbol{e}_{\perp p}v_\perp]|_*^2}{\left| pv_{||}\boldsymbol{n}\cdot\nabla\vartheta \frac{\mathrm{d}}{\mathrm{d}\vartheta}\left(\Omega_* + \frac{Iv_{||}}{\Omega}\frac{\partial\Omega}{\partial\psi}\right)\right|_*}, \quad (4.14)$$

where to focus on the effect due to radial drift departure from a flux surface we neglect the Doppler and drift broadening of the resonance as small by assuming $pI\Omega^{-1}v_{||}\partial\Omega/\partial\psi \gg k_{||}v_{||} \sim \boldsymbol{k}\cdot\boldsymbol{v}_d$ or $pB_t/B_p \gg k_{||}R \sim k_\perp\rho_p$. These inequalities are not well satisfied; but Doppler and drift broadening effects do not result in driven current in an up–down symmetric tokamak for an applied symmetric spectrum so are neglected to simplify the presentation. However, when a symmetric spectrum is launched in an up–down asymmetric tokamak an asymmetry in the wavenumber spectrum is introduced that may result in appreciable driven current. For trapped particles that do not pass through resonance ($B_0/B > \lambda > p\Omega/\omega$), $D = 0$.

In the preceding a finite poloidal gyroradius term is retained in the denominator as can be seen by using $B \simeq B_0(1 - \varepsilon\cos\vartheta)$ for $p = 1$ to obtain

$$\left| v_{||}\boldsymbol{n}\cdot\nabla\vartheta \frac{\mathrm{d}}{\mathrm{d}\vartheta}\left(\Omega_* + \frac{Iv_{||}}{\Omega}\frac{\partial\Omega}{\partial\psi}\right)\right|_* \simeq \frac{\varepsilon\omega v\sqrt{1-\lambda}}{qR_0}\left(1 + \frac{\sigma Iv\sqrt{1-\lambda}}{R_0 B_{p0} r\omega}\right) \equiv \frac{\omega}{\tau_{\mathrm{int}}}, \quad (4.15)$$

where $v_{||} \rightarrow \sigma v\sqrt{1-\lambda}$ and $R = R_0(1 + \varepsilon\cos\vartheta)$ with $\varepsilon = r/R_0 \ll 1$ and τ_{int} the interaction time with the applied rf field. We assume the resonance $\omega \simeq \Omega_*$ passes through the magnetic axis and allow finite

$$|Iv_{||}/RB_p r\Omega| \simeq |qv_{||}/\varepsilon r\omega| < 1. \quad (4.16)$$

In this large aspect ratio, on axis limit

$$\bar{D} \simeq \frac{\pi Z^2 e^2}{\varepsilon\omega M^2} \frac{H(1-\lambda)\sum_{\kappa,m,n} |\boldsymbol{e}_m \cdot [\boldsymbol{n}\sigma\sqrt{1-\lambda}J_1(w) + \boldsymbol{e}_{\perp 1}\lambda^{1/2}]|_*^2}{\sqrt{1-\lambda}\left(1 + \frac{\sigma Iv\sqrt{1-\lambda}}{RB_p r\omega}\right)\oint \mathrm{d}\vartheta/\xi}, \quad (4.17)$$

https://doi.org/10.1017/S0022377818001071 Published online by Cambridge University Press

where we let $\xi = \sqrt{1-\lambda B/B_0}$ and now $w = k_\perp \lambda^{1/2} v/\Omega$. The interaction time $\tau_{\rm int} \propto q/\varepsilon$ for the counter (co) travelling minorities that are closer to (further from) the magnetic axis is longer (shorter) and therefore more (less) heating occurs as shown schematically in figure 1. Both σ and I are signed quantities, so excess minority heating always occurs in the favourable counter-current direction. We account for the passing ions making two passes and the trapped ions making four passes through resonance during a complete poloidal circuit, and use

$$\oint d\vartheta/\xi = \frac{4}{\sqrt{2\varepsilon}} \begin{cases} \sqrt{1-\varepsilon+2\varepsilon\kappa^2}K(\kappa) & \text{trapped } (1 \geqslant \kappa^2 \geqslant 0) \\ \sqrt{(1-\varepsilon)k^2+2\varepsilon}K(k) & \text{passing } (1 \geqslant k^2 \geqslant 0), \end{cases} \tag{4.18}$$

where $\kappa^2 = k^{-2} = [1-(1-\varepsilon)\lambda]/2\varepsilon\lambda$, K is the complete elliptic integral of the first kind, and the trapped–passing boundary is at $\kappa^2 = 1 = k^{-2}$. When a trapped minority ion is unable to reach resonance, then $\bar{D} = 0$. Therefore, a Heaviside step function has been inserted in (4.17). The distinction between $\bar{\psi}_*$ and ψ is unimportant for r, R, $\boldsymbol{B}$, B_p, I, and $\Omega_0 \simeq \omega$, so no subscript appears.

Using pitch angle λ in (4.9) instead of magnetic moment gives

$$\frac{\partial}{\partial v} + \frac{p\Omega v}{\omega B}\frac{\partial}{\partial \mu_0} \to \frac{\partial}{\partial v} + \frac{2}{v}\left(\frac{p\Omega_0}{\omega} - \lambda\right)\frac{\partial}{\partial \lambda}, \tag{4.19}$$

where $p = 1$ and $\omega = \Omega_0$ for the resonance passing through the magnetic axis.

The next section considers the simplified limit for minority heating finite orbit current drive in which collisions dominate over quasilinear heating so that an adjoint method can be used to obtain explicit results.

5. A limiting diffusivity form for minority heating and current drive

For minority heating and current drive we need only keep $p = 1$ and the left-hand polarized wave (we set $\boldsymbol{e}_m \cdot \boldsymbol{n} = 0 = \boldsymbol{e}_m \cdot \boldsymbol{e}_-$), then for $w \ll 1$, $k_{||} v_{||} \to 0$, and $\boldsymbol{k} \cdot \boldsymbol{v}_d \to 0$, we are left with

$$D \simeq \frac{\pi Z^2 e^2 v_\perp^2}{8M^2 v^2} \sum_{\kappa,m,n} |\boldsymbol{e}_m \cdot \boldsymbol{e}_+|^2 \delta(\omega - \Omega - I\Omega^{-1} v_{||} \partial\Omega/\partial\psi). \tag{5.1}$$

Then for large aspect ratio with a resonance passing through the magnetic axis

$$\bar{D} \simeq \frac{\pi Z^2 e^2}{4\varepsilon\omega M^2} \frac{\lambda H(1-\lambda) \sum_{\kappa,m,n} |\boldsymbol{e}_m \cdot \boldsymbol{e}_+|_*^2}{\sqrt{1-\lambda}\left(1 + \frac{\sigma I v\sqrt{1-\lambda}}{RB_p r\omega}\right)\oint d\vartheta/\xi}. \tag{5.2}$$

In the absence of poloidal gyroradius effects $\bar{D}$ is an even function of $v_{||} = \sigma v\sqrt{1-\lambda}$.

We will next demonstrate that the finite orbit modification will lead to current drive for a symmetric heating spectrum. Actually, this is already clear from (5.2) since when $I > 0$ then there is more (less) heating of the $v_{||} < 0$ ($v_{||} > 0$) minorities, while if we reverse the toroidal magnetic field ($I < 0$) then there is more (less) heating of the $v_{||} > 0$ ($v_{||} < 0$) minorities. As a result, this symmetric spectrum driven minority current is always in the favourable counter-current direction!

https://doi.org/10.1017/S0022377818001071 Published online by Cambridge University Press

For minority ion heating and current drive an approximate collision operator for the energetic minorities is obtained by performing speed expansions of the full unlike Fokker–Planck collision operator for $v_e^2 = 2T_e/m \gg v^2 \gg v_i^2 = 2T_i/M_i$. We define the slowing down time by electron drag as

$$\tau_s = \frac{3MT_e^{3/2}}{4(2\pi m)^{1/2}Z^2e^4n_e\ell n\Lambda}, \tag{5.3}$$

with M and Z the minority mass and charge number. We also define the critical speed v_c at which electron and ion drag are equal by

$$v_c^3 = \frac{3\pi^{1/2}T_e^{3/2}}{(2m)^{1/2}n_e}\sum_i \frac{Z_i^2 n_i}{M_i}, \tag{5.4}$$

and a speed below which, and in the vicinity of, pitch scattering must be retained by

$$v_\lambda^3 = \frac{3\pi^{1/2}T_e^{3/2}}{(2m)^{1/2}M_m n_e}\sum_i Z_i^2 n_i, \tag{5.5}$$

where the sums are over all background ion species. Then the speed expansions give the non-self-adjoint vector form

$$C\{f_0\} = \frac{1}{\tau_s}\nabla_v \cdot \left[\left(\boldsymbol{v}f_0 + \frac{T_e}{M}\nabla_v f_0\right) + \frac{v_c^3}{v^3}\left(\boldsymbol{v}f_0 + \frac{\bar{T}_i}{M}\nabla_v f_o\right) + \frac{v_\lambda^3}{2v^3}(v^2 \overleftrightarrow{I} - \boldsymbol{v}\boldsymbol{v}) \cdot \nabla_v f_0\right], \tag{5.6}$$

with

$$\bar{T}_i = \left(\sum_i Z_i^2 n_i T_i/M_i\right) \Big/ \left(\sum_i Z_i^2 n_i/M_i\right). \tag{5.7}$$

The preceding collision operator is not quite self-adjoint as it relaxes the lower speed minorities to a Maxwellian at the effective ion temperature $\bar{T}_i$, and the more energetic minorities toward a Maxwellian at the electron temperature. The ion drag time and pitch angle scattering times are τ_s/v_c^3 and τ_s/v_λ^3, and $v_e^3 \gg v_c^3 \sim v_\lambda^3 \gg v_i^3$.

If we simplify by assuming $\bar{T}_i = T_e$ then the collision operator vanishes for a Maxwellian minority distribution function and is self-adjoint. This feature suggests an adjoint solution method to demonstrate that parallel current can be driven by a symmetric spectrum of ion cyclotron waves. To begin we let $f_0 = f_0^{(0)} + f_0^{(1)} + \cdots$ with $f_0^{(0)} \gg f_0^{(1)}$ and assume that to lowest order

$$(v_{||}\boldsymbol{n} + \boldsymbol{v}_d) \cdot \nabla f_0^{(0)} = C\{f_0^{(0)}\}. \tag{5.8}$$

Transit averaging gives a solubility constraint

$$\overline{C\{f_0^{(0)}\}} = 0 \tag{5.9}$$

that can only be satisfied by a Maxwellian,

$$f_0^{(0)} = f_M = n_m(M/2\pi T_e)^{3/2}e^{-Mv^2/2T_e}, \tag{5.10}$$

https://doi.org/10.1017/S0022377818001071 Published online by Cambridge University Press

with n_m the minority density. For a Maxwellian, $C\{f_M\}=0$, so we must also satisfy

$$(v_{||}\boldsymbol{n}+\boldsymbol{v}_d)\cdot\nabla f_M=0. \tag{5.11}$$

Consequently, to remain Maxwellian, f_M cannot depend on $\bar{\psi}_*$. Any spatial variation of n_m and T_e in $f_M(v)$ must be weak compared to a poloidal minority gyroradius and lead to neoclassical effects that are not of interest here. Cottrell & Start (1991) consider the minority heating when minority drift departures off a flux surface are on the scale of the background radial variation of the slowing down time. They ignore the symmetric spectrum current drive associated with the distinction between flux and drift surfaces as they pass through resonance. However, for the large departures they consider, the asymmetry in the electron drag may also result in a symmetric spectrum driven counter-current as will be estimated later in this section.

Letting $\tilde{f}=f_0^{(1)}$ to streamline the notation, the next order equation becomes

$$(v_{||}\boldsymbol{n}+\boldsymbol{v}_d)\cdot\nabla\tilde{f}-C\{\tilde{f}\}=Q\{f_M\}, \tag{5.12}$$

where the self-adjoint form for C is

$$C\{\tilde{f}\}=\frac{1}{\tau_s}\nabla_v\cdot\left\{\frac{v^3+v_c^3}{v^3}\left[\frac{T_e}{M}f_M\nabla_v\left(\frac{\tilde{f}}{f_M}\right)\right]+\frac{v_\lambda^3 f_M}{2v^3}(v^2\overleftrightarrow{I}-\boldsymbol{v}\boldsymbol{v})\cdot\nabla_v\left(\frac{\tilde{f}}{f_M}\right)\right\}. \tag{5.13}$$

To lowest order we assume

$$(v_{||}\boldsymbol{n}+\boldsymbol{v}_d)\cdot\nabla\tilde{f}=0, \tag{5.14}$$

which allows poloidal gyroradius scale spatial variation in $\tilde{f}$ only via $\bar{\psi}_*$. Transit averaging the next order equation gives the solubility constraint

$$\overline{C\{\tilde{f}\}}+\overline{Q\{f_M\}}=0; \tag{5.15}$$

a difficult equation to solve.

To evaluate the symmetric spectrum parallel current driven by finite poloidal gyroradius effects we introduce the modified adjoint equation

$$(v_{||}\boldsymbol{n}+\boldsymbol{v}_d)\cdot\nabla\tilde{g}+C\{\tilde{g}\}=-Bv_{||}f_M/I(\psi), \tag{5.16}$$

and use a finite orbit generalization of the technique of Antonsen & Chu (1982). Multiplying the $\tilde{f}$ equation by $\tilde{g}/f_M$ and the $\tilde{g}$ equation by $\tilde{f}/f_M$, integrating over velocity space, flux surface averaging and adding gives

$$\left\langle B\int \mathrm{d}^3v\,v_{||}\tilde{f}\right\rangle = I\left\langle\int \mathrm{d}^3v\,\tilde{g}f_M^{-1}Q\{f_M\}\right\rangle, \tag{5.17}$$

where we used the self-adjointness of C, and (2.9). In the absence of finite poloidal gyroradius modifications and for a symmetric spectrum, $\bar{D}$ and lowest order $\tilde{f}$ would be even functions of $v_{||}$ and lowest order $\tilde{g}$ would be an odd function of $v_{||}$.

It is simpler to solve the $\tilde{g}$ equation than the equation for $\tilde{f}$. To lowest order

$$(v_{||}\boldsymbol{n}+\boldsymbol{v}_d)\cdot\nabla\tilde{g}=v_{||}\boldsymbol{n}\cdot\nabla\vartheta\,\partial\tilde{g}/\partial\vartheta|_{\bar{\psi}_*}=0, \tag{5.18}$$

https://doi.org/10.1017/S0022377818001071 Published online by Cambridge University Press

so any spatial variation of $\tilde{g}$ is through $\bar{\psi}_*$. Transit averaging the next order equation gives the solubility constraint

$$\overline{C\{\tilde{g}\}} = -\overline{Bv_{||}} f_M / I. \tag{5.19}$$

For the trapped particles $\overline{Bv_{||}} = 0$, which gives $\tilde{g}_t = 0$. For the passing particles we can replace the transit averages by a flux surface averages. Then we need only solve

$$I\langle Bv_{||}^{-1} C\{\tilde{g}_p\}\rangle = -\langle B^2\rangle f_M, \tag{5.20}$$

where we have used $\langle (B/v_{||})[v_{||}\boldsymbol{n} + \Omega^{-1} v_{||} \nabla \times (v_{||}\boldsymbol{n})] \cdot \nabla \tilde{g}_p \rangle = 0$.

We simplify further by assuming $v_m^3 \equiv (2T_e/M)^{3/2} \ll v^3 \lesssim v_c^3 \sim v_\lambda^3 \ll (2T_e/m)^{3/2} \equiv v_e^3$, then we need to solve

$$\frac{\sigma I T_e \langle B/\xi\rangle}{\tau_s M v^3 f_M} \frac{\partial}{\partial v}\left[\frac{(v^3 + v_c^3) f_M}{v} \frac{\partial}{\partial v}\left(\frac{\tilde{g}_p}{f_M}\right)\right] + \frac{2\sigma I v_\lambda^3 B_0}{\tau_s v^4 f_M} \frac{\partial}{\partial \lambda}\left(\lambda\langle\xi\rangle \frac{\partial \tilde{g}_p}{\partial \lambda}\right) = -\langle B^2\rangle. \tag{5.21}$$

If we use the $\varepsilon \ll 1$ approximations $\langle\xi\rangle \simeq \sqrt{1-\lambda}$ and $\langle B/\xi\rangle \simeq B_0/\sqrt{1-\lambda}$, then we may take $\tilde{g}_p = \sqrt{1-\lambda} G_p(v)$ to find

$$\begin{aligned} \frac{T_e}{M}\frac{\partial}{\partial v}\left[\frac{(v^3 + v_c^3) f_M}{v}\frac{\partial}{\partial v}\left(\frac{G_p}{f_M}\right)\right] - \frac{v_\lambda^3}{v} G_p &= -\sigma I^{-1} B_0 \tau_s v^3 f_M \\ &= \frac{\sigma B_0 \tau_s T_e}{IM}\frac{\partial}{\partial v}\left[\left(v^2 + \frac{2T_e}{M}\right) f_M\right], \end{aligned} \tag{5.22}$$

where we recall $\langle B^2\rangle = B_0^2$. For $v_\lambda^3 \to 0$ we see that

$$\frac{G_p}{f_M} \to \frac{\sigma B_0 \tau_s}{I}\int_0^v \mathrm{d}v \frac{v(v^2 + v_m^2)}{(v^3 + v_c^3)} \simeq \frac{\sigma B_0 \tau_s v^4}{4 I v_c^3}. \tag{5.23}$$

Retaining the pitch angle scattering term for $v_m^3 \ll v^3 \ll v_c^3 \sim v_\lambda^3$ we find

$$\tilde{g}_p = \sqrt{1-\lambda} G_p \simeq \frac{\sigma B_0 \tau_s v^4 f_M \sqrt{1-\lambda}}{I(4v_c^3 + v_\lambda^3)}. \tag{5.24}$$

To evaluate the current we use $\partial \tilde{g}_p / \partial \vartheta = 0$ to rewrite (5.17) as

$$\left\langle B\int \mathrm{d}^3 v v_{||} \tilde{f}\right\rangle = I\int \mathrm{d}^3 v \frac{v_{||}}{B f_M}\left\langle \tilde{g}_p \frac{B}{v_{||}} Q\{f_M\}\right\rangle \simeq I\int \mathrm{d}^3 v \frac{v_{||}\tilde{g}_p}{B f_M}\left\langle \frac{B}{v_{||}} Q\{f_M\}\right\rangle, \tag{5.25}$$

with

$$\left\langle \frac{B}{v_{||}} Q\{f_M\}\right\rangle = \frac{1}{v}\left[\frac{\partial}{\partial v} + \frac{2}{v}(1-\lambda)\frac{\partial}{\partial \lambda}\right]\left(\left\langle \frac{BD}{v_{||}}\right\rangle v \frac{\partial f_M}{\partial v}\right). \tag{5.26}$$

Then recalling $B_0 \mathrm{d}^3 v |v_{||}| \to 2\pi B v^3 \,\mathrm{d}v\,\mathrm{d}\lambda$ and $\langle BD/v_{||}\rangle|_{\lambda=0} = 0$, integrating by parts gives

$$\left\langle B\int \mathrm{d}^3 v v_{||}\tilde{f}\right\rangle = \frac{3MI}{T_e}\int \mathrm{d}^3 v \frac{v_{||}\tilde{g}_p}{B}\left\langle \frac{BD}{v_{||}}\right\rangle, \tag{5.27}$$

https://doi.org/10.1017/S0022377818001071 Published online by Cambridge University Press

where the finite orbit effect enters in the denominator of

$$\left\langle \frac{BD}{v_{||}} \right\rangle \simeq \frac{D_0 B_0 \lambda}{8\varepsilon\sigma v\sqrt{1-\lambda}\left(1+\dfrac{\sigma I v\sqrt{1-\lambda}}{RB_p r\omega}\right)}, \tag{5.28}$$

with D_0 and the quiver speed $v_{\rm quiv}$ defined by

$$\frac{D_0}{\omega} \equiv v_{\rm quiv}^2 \equiv \frac{Z^2 e^2}{M^2\omega^2} \sum_{\kappa,m,n} |\boldsymbol{e}_m \cdot \boldsymbol{e}_+|_*^2. \tag{5.29}$$

Substituting in and summing over both signs of σ gives

$$\left\langle B \int \mathrm{d}^3 v v_{||} \tilde{f} \right\rangle \simeq \frac{-3\pi I M B_0 \tau_s D_0}{2\varepsilon T_e R B_p r\omega (4v_c^3 + v_\lambda^3)} \int_0^\infty \mathrm{d}v v^7 f_M \int_0^1 \mathrm{d}\lambda \frac{\lambda\sqrt{1-\lambda}}{[1-(qv\sqrt{1-\lambda}/\varepsilon r\omega)^2]}. \tag{5.30}$$

Assuming $(qv/\varepsilon r\omega)^2 \ll 1$, we find the minority parallel current driven by the symmetric spectrum to be

$$J_{\rm min} = ZeB_0^{-1} \left\langle B \int \mathrm{d}^3 v v_{||} \tilde{f} \right\rangle \simeq -\frac{12 Z e n_m v_m^3 v_{\rm quiv}^2 \tau_s I}{5\pi^{1/2}(4v_c^3 + v_\lambda^3)\varepsilon r R B_p}, \tag{5.31}$$

where we use $\pi^{3/2}\int_0^\infty \mathrm{d}v v^7 f_M = 3 n_m v_m^5$ and $\int_0^1 \mathrm{d}\lambda\lambda\sqrt{1-\lambda} = 4/15$. For 3.5 MeV alphas in a 5 T field, $v/\omega \sim 5$ cm.

The bootstrap current is

$$J_{\rm bs} \sim Z_i e n_e v_i (q v_i / \varepsilon^{1/2} \Omega_i a), \tag{5.32}$$

with $v_i^2 = 2T_i/M_i$. The ratio gives

$$\frac{J_{\rm min}}{J_{\rm bs}} \sim \frac{Z M_i a n_m v_m v_{\rm quiv}^2 \omega\tau_s}{Z_i M \varepsilon^{3/2} r n_e v_c^3} \sim \frac{Z M_i n_m a}{Z_i M \varepsilon^{3/2} n_e r}\left(\frac{\omega\tau_s v_{\rm quiv}^2}{v_c^3/v_m}\right), \tag{5.33}$$

with $\Omega_i \simeq \omega$. Next we estimate this ratio to determine when the size of the symmetric spectrum current drive becomes interesting.

For the minority ions to be a lowest order Maxwellian collisions must dominate. Using (5.13) with $v \sim v_m$ gives $\bar{C}\{\tilde{f}\} \sim \tilde{f} v_c^3/v_m^3\tau_s$. Using (5.26) and (5.27) gives the estimate $\bar{Q}\{f_M\} \sim f_M D/v_m^2 \sim f_M D_0/\varepsilon v_m^2$. As a result, we expect (5.15) to give

$$\tilde{f}/f_M \sim v_m \tau_s D_0/\varepsilon v_c^3 \sim \omega\tau_s v_{\rm quiv}^2 v_m/\varepsilon v_c^3 \ll 1. \tag{5.34}$$

This estimate suggests weak symmetric spectrum minority current drive. However, balancing electron drag and minority heating gives $\omega\tau_s v_{\rm quiv}^2 \sim \varepsilon v_m^2$, with $\omega\tau_s v_{\rm quiv}^2 \gg \varepsilon v_m^2$ generating highly non-Maxwellian minority distributions, as found by Stix (1975) and as seen from other bi-Maxwellian forms (Catto & Myra 1992; Catto, Myra & Russell 1994). For example, it may be possible that alternate estimates such as $\bar{Q}\{\tilde{f}\} \sim \tilde{f} D_0/\varepsilon v_c^2$ and $\bar{C}\{\tilde{f}\} \sim \tilde{f}/\tau_s$ become appropriate for $v \sim v_c$, giving $\omega\tau_s v_{\rm quiv}^2 \sim \varepsilon v_c^2$.

https://doi.org/10.1017/S0022377818001071 Published online by Cambridge University Press

Then the driven current is v_c^3/v_m^3 larger, and significant levels of symmetric spectrum current drive of order $J_{\min} \sim Zen_m v_{\rm quiv}^2 \tau_s q/\varepsilon^2 r \sim Zen_m v_c^2 q/\varepsilon\omega r$ might occur for a large minority fraction near the magnetic axis since $J_{\min}/J_{\rm bs} \sim (Zn_m a/Z_i \varepsilon^{1/2} n_e r)(v_c^2/v_i^2)$. Also, the symmetric spectrum current might be enhanced slightly by allowing larger finite orbit effects with $\eta^2 \equiv (qv/\varepsilon r\omega)^2 \to 1$ at resonance in (5.30). We can estimate this effect using

$$\int_0^1 {\rm d}\lambda \frac{\lambda\sqrt{1-\lambda}}{[1-\eta^2(1-\lambda)]} = 2\int_0^1 {\rm d}x \frac{x^2(1-x^2)}{(1-\eta^2 x^2)} = \frac{2}{\eta^4} - \frac{4}{3\eta^2} + \frac{1}{\eta^3}\left(1-\frac{1}{\eta^2}\right)\ell n\left(\frac{1+\eta}{1-\eta}\right), \tag{5.35}$$

which for $\eta^2 \to 1$ goes to 2/3 so is 5/2 bigger. It is perhaps possible that, with all these embellishments, minority current drive by a symmetric spectrum might become viable. A substantial simulation effort will be required to determine if this is the case. One possibility is to consider an energetic helium three minority in a deuterium majority plasma to determine whether significant overall co-current is driven.

To verify that our evaluation of the amount of current that can be driven by a symmetric spectrum is sensible we can use (5.15) to estimate

$$\tilde{f}/f_M \sim (v_m \tau_s D_0/\varepsilon v_c^3)[1 + O(qv_m/\varepsilon r\omega)] \sim (\omega\tau_s v_{\rm quiv}^2 v_m/\varepsilon v_c^3)[1 + O(qv_m/\varepsilon r\omega)] \ll 1, \tag{5.36}$$

where we keep the finite orbit correction of order $qv/\varepsilon r\omega$ to drive a current with a symmetric spectrum. As result, we obtain an estimate consistent with (5.31), namely

$$J_{\min} = ZeB_0^{-1}\left\langle B\int {\rm d}^3 v v_{||}\tilde{f}\right\rangle \sim Zen_m v_m^3 v_{\rm quiv}^2 \tau_s q/v_c^3 \varepsilon^2 r. \tag{5.37}$$

To understand the direction of symmetric spectrum driven current we first note that from (5.2) or (5.27) asymmetric heating occurs due to the finite orbit effect. When $Iv_{||} = \sigma Iv\sqrt{1-\lambda} < 0$ the minorities with $Iv_{||} < 0$ are heated more than those with $Iv_{||} > 0$. We assume the ohmic current is in the positive $\nabla\zeta$ direction so that $B_p > 0$ always. Consequently, when $I > 0$ in (2.2) the $v_{||} < 0$ minorities are heated more than those with $v_{||} > 0$. As a result, the symmetric spectrum current driven is counter-current (in the direction opposite to both the ohmic current and the toroidal magnetic field). Moreover, when $I < 0$, the $v_{||} > 0$ minorities are heated more and the symmetric spectrum driven current remains counter-current (opposite to the ohmic direction, but in the direction of the toroidal magnetic field). This behaviour is consistent with (5.31).

The Cottrell & Start (1991) asymmetric electron drag mechanism also heats $v_{||} < 0$ ($v_{||} > 0$) minorities more than those with $v_{||} > 0$ ($v_{||} < 0$) for $I > 0$ ($I < 0$) so is also expected to result in symmetric spectrum minority current drive. In this case the replacement

$$Iv_{||}/R_0 B_{p0} r\omega \to (Iv_{||}/\omega\tau_s)\partial\tau_s/\partial\psi \tag{5.38}$$

in (5.31) results in a counter-current

$$J_{\min} = ZeB_0^{-1}\left\langle B\int {\rm d}^3 v v_{||}\tilde{f}\right\rangle \simeq \frac{12Zen_m v_m^3 v_{\rm quiv}^2 I}{5\pi^{1/2}(4v_c^3 + v_\lambda^3)\varepsilon}\frac{\partial\tau_s}{\partial\psi}, \tag{5.39}$$

https://doi.org/10.1017/S0022377818001071 Published online by Cambridge University Press

as we expect $\partial\tau_s/\partial\psi < 0$. Further discussion of their mechanism will be given in the next section where we consider whether symmetric spectrum current drive can affect alphas significantly.

When the spectrum is symmetric and the species being heated Maxwellian to lowest order, then the flux surface averaged minority heating power absorbed is

$$P = (M/2)\left\langle \int \mathrm{d}^3 v v^2 Q\{f_M\}\right\rangle \simeq M^2 T^{-1}\left\langle \int \mathrm{d}^3 v \boldsymbol{v}\cdot\overleftrightarrow{D}\cdot\boldsymbol{v} f_M\right\rangle$$
$$= M^2 T^{-1} B^{-1}\int \mathrm{d}^3 v v_{||} v^2 f_M \langle BD/v_{||}\rangle, \tag{5.40}$$

where we use the form $Q\{f_0\} = \boldsymbol{\nabla}_v\cdot(\overleftrightarrow{D}\cdot\boldsymbol{\nabla}_v f_0)$ from Catto *et al.* (2017), keep only a single wave frequency and take $p=1$. Inserting (5.27), using $B_0\mathrm{d}^3 v|v_{||}| \to 2\pi B v^3\,\mathrm{d}v\,\mathrm{d}\lambda$ and summing over both signs of $v_{||}$ yields

$$P \simeq \frac{\pi M^2 D_0}{4\varepsilon T_e}\int_0^\infty \mathrm{d}v v^4 f_M \int_0^{1-\varepsilon}\mathrm{d}\lambda \frac{\lambda}{\sqrt{1-\lambda}} \simeq \frac{n_m M v_{\mathrm{quiv}}^2 \omega}{\pi\varepsilon}, \tag{5.41}$$

where we assume on axis heating and $(qv/\varepsilon r\omega)^2 \ll 1$. No additional power is required to drive symmetric spectrum current as it is simply an inevitable side effect.

In the next section we consider the case when the minority is the energetic alphas born in deuterium–tritium reactions so the deuterium is the minority being heated and the alphas are the minority in which symmetric spectrum current is driven.

6. Symmetric spectrum current drive by alphas

The species with the largest finite poloidal gyroradius and the highest energy is the alpha particles. We can modify the treatment of the previous section to see whether a symmetric spectrum will drive appreciable alpha current. This current could be generated prior to ignition, by using deuterium (D) as the heated minority in a tritium (T) majority plasma, as the energetic minority alphas and the D have the same charge over mass ratio. The symmetric spectrum would be first used to heat the minority D to fusion temperatures, and then as alphas are produced the symmetric spectrum could drive alpha current by taking advantage of their large poloidal gyroradius and weak collisionality.

The alpha calculation is somewhat different than the minority calculation of the previous section. The most obvious difference is that an alpha source is needed in (5.8) so it is replaced by

$$(v_{||}\boldsymbol{n} + \boldsymbol{v}_d)\cdot\boldsymbol{\nabla} f_0^{(0)} = C\{f_0^{(0)}\} + \frac{S\delta(v-v_0)}{4\pi v^2}, \tag{6.1}$$

where the alphas of mass M and charge number Z are born with birth speed v_0. The coefficient of the $\delta(v-v_0)$ function is the fusion birth rate for alphas:

$$S = S(\psi) = n_T(\psi) n_D(\psi)\langle\sigma v\rangle_{DT}, \tag{6.2}$$

with the flux function $\langle\sigma v\rangle_{DT}$ the D-T reaction rate.

The collision operator used for alphas is a simpler version of (5.6) since we are now interested in $v_e^2 \gg v_0^2 \sim v^2 \gg v_i^2$:

$$C\{f_0\} = \frac{1}{\tau_s}\boldsymbol{\nabla}_v\cdot\left[\left(\frac{v^3+v_c^3}{v^3}\right)\boldsymbol{v} f_0 + \frac{v_\lambda^3}{2v^3}(v^2\overleftrightarrow{I} - \boldsymbol{v}\boldsymbol{v})\cdot\boldsymbol{\nabla}_v f_0\right], \tag{6.3}$$

https://doi.org/10.1017/S0022377818001071 Published online by Cambridge University Press

where $f_0 = f_0^{(0)} + f_0^{(1)} + \cdots$. We can assume the spatial variation of the alphas born on surfaces of constant pressure is slow compared to a typical alpha poloidal gyroradius as the source rate S and the alpha slowing down time τ_s depend on the background species. As a result, (6.1) is satisfied by taking

$$f_0^{(0)} = f_s(v) = \frac{S\tau_s H(v_0 - v)}{4\pi(v^3 + v_c^3)}, \tag{6.4}$$

which is the usual alpha slowing down tail distribution function with $H(v_0 - v)$ the Heaviside step function. The density of slowing down alphas is

$$n_s = \int \mathrm{d}^3 v f_s = S\tau_s \int_0^{v_0} \frac{\mathrm{d}v v^2}{(v^3 + v_c^3)} = \frac{S\tau_s}{3} \ell n[1 + (v_0^3/v_c^3)] \simeq S\tau_s \ell n(v_0/v_c), \tag{6.5}$$

where we assume $v_0^3 \gg v_c^3$ as is the case for D–T fusion reaction. The alphas are a trace population since $n_s/n_e \sim T_i/Mv_0^2 \ll 1$, based on the estimate $n_s M v_0^2 \sim n_e T_i$.

The next order equations are similar to the minority case except the Maxwellian f_M is replaced by f_s in (5.15) to obtain

$$\overline{C\{\tilde{f}\}} + \overline{Q\{f_s\}} = 0. \tag{6.6}$$

To get an estimate for the alphas when electron drag dominates we further approximate C by keeping only the drag terms,

$$C\{f\} = \frac{1}{\tau_s} \nabla_v \cdot \left[\left(\frac{v^3 + v_c^3}{v^3} \right) \boldsymbol{v} f \right] = \frac{S}{4\pi} \nabla_v \cdot \left[\frac{\boldsymbol{v} f}{v^3 f_s} H(v_0 - v) \right], \tag{6.7}$$

where $\nabla_v \cdot (\boldsymbol{v} v^{-3}) = 4\pi\delta(\boldsymbol{v})$. Then we let $f_0^{(1)} = \tilde{f}$ and consider

$$(v_{||}\boldsymbol{n} + \boldsymbol{v}_d) \cdot \nabla \tilde{f} - C\{\tilde{f}\} = Q\{f_s\}, \tag{6.8}$$

and the modified adjoint equation required to treat electron drag,

$$(v_{||}\boldsymbol{n} + \boldsymbol{v}_d) \cdot \nabla \tilde{g} - C\{\tilde{g}\} = -Bv_{||} f_s / I, \tag{6.9}$$

where the sign of C has changed from (5.16). Multiplying the $\tilde{f}$ equation by $(\tilde{g}/f_s)H(v_0 - v)$ and the $\tilde{g}$ equation by $(\tilde{f}/f_s)H(v_0 - v)$, integrating over velocity space, flux surface averaging and adding gives

$$\left\langle B \int \mathrm{d}^3 v v_{||} \tilde{f} H(v_0 - v) \right\rangle = I \left\langle \int \mathrm{d}^3 v \frac{\tilde{g}}{f_s} H(v_0 - v) Q\{f_s\} \right\rangle + IS \left\langle \int \mathrm{d}^3 v f_s^{-2} \tilde{g} \tilde{f} \delta(\boldsymbol{v}) \right\rangle, \tag{6.10}$$

where we use

$$\begin{aligned} 4\pi S^{-1} f_s^{-1} H(v_0 - v)[\tilde{g} C\{\tilde{f}\} + \tilde{f} C\{\tilde{g}\}] \; = \; & \nabla_v \cdot [\boldsymbol{v} v^{-3} f_s^{-2} \tilde{g} \tilde{f} H^2(v_0 - v)] \\ & + f_s^{-2} \tilde{g} \tilde{f} H^2(v_0 - v) \nabla_v \cdot (\boldsymbol{v} v^{-3}). \end{aligned} \tag{6.11}$$

To lowest order (5.18) still holds. To next order we must solve

$$I \langle B / v_{||} \rangle C\{\tilde{g}\} = \langle B^2 \rangle f_s \tag{6.12}$$

https://doi.org/10.1017/S0022377818001071 Published online by Cambridge University Press

for the passing with the drag approximation to the collision operator, giving

$$\frac{1}{\tau_s v^2}\frac{\partial}{\partial v}[(v^3+v_c^3)\tilde{g}_p]=\frac{\langle B^2\rangle f_s}{I\langle B/v_{||}\rangle}, \tag{6.13}$$

where $\tilde{g}$ vanishes for the trapped ($\tilde{g}_t=0$) and we are assuming $v^3\gg v_c^3\sim v_\lambda^3$. For smaller v pitch angle scattering also enters, but $\tilde{g}_p(v=0)=0$ so the delta function term in (6.10) vanishes. Integrating (6.13) from v to v_0 to make $\tilde{g}_p(v>v_0)=0$, we find

$$\tilde{g}_p=-\frac{\sigma\tau_s\langle B^2\rangle f_s}{I\langle B/\xi\rangle}\int_v^{v_0}\frac{\mathrm{d}uu^3}{u^3+v_c^3}\simeq-\sigma I^{-1}\tau_s B_0 f_s\sqrt{1-\lambda}\int_v^{v_0}\frac{\mathrm{d}uu^3}{u^3+v_c^3}, \tag{6.14}$$

where we again assume $\varepsilon\ll 1$.

Using

$$\left\langle\frac{B}{v_{||}}Q\{f_s\}\right\rangle=\frac{1}{v}\left[\frac{\partial}{\partial v}+\frac{2}{v}(1-\lambda)\frac{\partial}{\partial\lambda}\right]\left(\left\langle\frac{BD}{v_{||}}\right\rangle v\frac{\partial f_s}{\partial v}\right), \tag{6.15}$$

and $\tilde{f}(v>v_0)=0$ we find

$$\left\langle B\int \mathrm{d}^3v v_{||}\tilde{f}\right\rangle=I\int \mathrm{d}^3v\frac{v_{||}\tilde{g}_p}{Bf_s}\left\langle\frac{B}{v_{||}}Q\{f_s\}\right\rangle=-I\int \mathrm{d}^3v\frac{v_{||}}{Bv}\left\langle\frac{BD}{v_{||}}\right\rangle\frac{\partial f_s}{\partial v}\frac{\partial}{\partial v}\left(\frac{v\tilde{g}_p}{f_s}\right). \tag{6.16}$$

Inserting $\tilde{g}_p$ and $\langle BD/v_{||}\rangle$, and summing over both signs of σ gives

$$\begin{aligned}B_0^{-1}\left\langle B\int \mathrm{d}^3v v_{||}\tilde{f}\right\rangle=&-\frac{\pi ID_0\tau_s}{2\varepsilon r\omega RB_p}\int_0^\infty \mathrm{d}vv^3\frac{\partial f_s}{\partial v}\frac{\partial}{\partial v}\\&\times\left(v\int_v^{v_0}\frac{\mathrm{d}uu^3}{u^3+v_c^3}\right)\int_0^1\frac{\mathrm{d}\lambda\lambda\sqrt{1-\lambda}}{1-(Iv/r\omega RB_p)^2(1-\lambda)},\end{aligned} \tag{6.17}$$

which for $(qv/\varepsilon r\omega)^2\ll 1$ reduces to

$$B_0^{-1}\left\langle B\int \mathrm{d}^3v v_{||}\tilde{f}\right\rangle=-\frac{2\pi ID_0\tau_s}{15\varepsilon r\omega RB_p}\int_0^\infty \mathrm{d}vv^2\frac{\partial f_s}{\partial v}\frac{\partial}{\partial v}\left[v\int_v^{v_0}\mathrm{d}u\frac{u^3}{u^3+v_c^3}\right]. \tag{6.18}$$

Using

$$\frac{\partial f_s}{\partial v}=-\frac{3v^2f_s}{(v^3+v_c^3)}-\frac{S\tau_s\delta(v-v_0)}{4\pi(v^3+v_c^3)} \tag{6.19}$$

along with

$$\int_0^\infty \mathrm{d}vv^2\frac{\delta(v-v_0)}{v^3+v_c^3}\frac{\partial}{\partial v}\left[v\int_v^{v_0}\mathrm{d}u\frac{u^3}{u^3+v_c^3}\right]=\frac{-v_0^6}{(v_0^3+v_c^3)^2}\simeq-1 \tag{6.20}$$

https://doi.org/10.1017/S0022377818001071 Published online by Cambridge University Press

and

$$\int_0^\infty \mathrm{d}v \frac{v^4 f_s}{(v^3+v_c^3)} \frac{\partial}{\partial v}\left[v\int_v^{v_0} \mathrm{d}u \frac{u^3}{u^3+v_c^3}\right] \simeq \int_{v_c}^{v_0} \mathrm{d}v v f_s(v_0-2v)$$
$$\simeq -\frac{S\tau_s}{4\pi}\left[1+2\ell n\left(\frac{v_0}{v_c}\right)\right], \qquad (6.21)$$

we find

$$\int_0^\infty \mathrm{d}v v^2 \frac{\partial f_s}{\partial v}\frac{\partial}{\partial v}\left[v\int_v^{v_0} \mathrm{d}u \frac{u^3}{u^3+v_c^3}\right] \simeq -\frac{S\tau_s}{2\pi}\left[\ell n\left(\frac{v_0}{v_c}\right)+1\right]. \qquad (6.22)$$

As a result, the symmetric spectrum driven alpha current is

$$J_{\text{alpha}} = ZeB_0^{-1}\left\langle B\int \mathrm{d}^3 v v_{||}\tilde{f}\right\rangle \simeq -\frac{Zen_s ID_0\tau_s}{15\varepsilon r\omega RB_p}. \qquad (6.23)$$

Assuming $Mn_s \ll M_D n_D$ and $Z^2 n_s \ll Z_D^2 n_D$, we can generalize (1.7) to find $J_{||} \simeq -J_{\text{alpha}} \simeq -Zen_m V_{||m}$ by assuming the parallel velocities of the deuterium and tritium are equal due to the friction between them and $n_\alpha \ll n_D < n_T$.

For alpha heating we expect $n_s/n_e \sim v_i^2/v_0^2 \ll 1$. Comparing this alpha current to the bootstrap current we expect

$$\frac{J_{\text{alpha}}}{J_{\text{bs}}} \sim \frac{Zn_s v_{\text{quiv}}^2 \omega\tau_s a}{Z_i n_e v_i^2 \varepsilon^{3/2} r} \sim \frac{Zv_{\text{quiv}}^2 \omega\tau_s a}{Z_i v_0^2 \varepsilon^{3/2} r}. \qquad (6.24)$$

Therefore, $\omega\tau_s v_{\text{quiv}}^2 \sim \varepsilon v_0^2 \gg \varepsilon v_i^2$ is required to drive substantial symmetric spectrum alpha current. The alpha birth speed for D–T fusion is $v_0 \simeq 1.3\times 10^9$ cm sec^{-1}, while at 10 keV, $v_i \simeq 10^8$ cm sec^{-1} and $v_0/v_c \simeq 3$ for a deuterium density approaching the tritium density. Consequently, for a Stix parameter $\omega\tau_s v_{\text{quiv}}^2/\varepsilon v_i^2 \sim 100$ it may be possible to drive significant symmetric spectrum alpha current, especially near the axis.

We can check that (6.23) is reasonable by estimating $\bar{Q}\{f_s\} \sim f_s D/v_0^2 \sim f_s D_0/\varepsilon v_0^2$ and $\bar{C}\{\tilde{f}\} \sim \tilde{f}/\tau_s$ to find $\tilde{f}/f_s \sim \tau_s D_0/\varepsilon v_0^2 \sim \omega\tau_s v_{\text{quiv}}^2/\varepsilon v_0^2 \ll 1$. As a result,

$$J_{\text{alpha}} \sim Zen_s v_0(\omega\tau_s v_{\text{quiv}}^2/\varepsilon v_0^2)(qv_0/\varepsilon\omega r) = Zen_s\tau_s v_{\text{quiv}}^2 q/\varepsilon^2 r, \qquad (6.25)$$

in agreement with (6.23).

The symmetric spectrum alpha counter-current drive associated with the electron drag asymmetry mechanism considered by Cottrell & Start (1991) can be estimated by making the replacement $\tau_s/\langle B/\xi\rangle \to 1/\langle B/\xi\tau_s\rangle \simeq B_0^{-1}\sqrt{1-\lambda}/\langle 1/\tau_s\rangle$ in (6.13) and (6.14) and then expanding $\tau_s(\psi)$ about $\tau_s(\psi_*)$. The result will be that $qv_0/\varepsilon\omega r$ in (6.25) is replaced by $(qv_0/\varepsilon\omega)\tau_s^{-1}\partial\tau_s/\partial r$. More precisely, the preceding means that (6.23) becomes

$$J_{\text{alpha}} = ZeB_0^{-1}\left\langle B\int \mathrm{d}^3 v v_{||}\tilde{f}\right\rangle \simeq -\frac{Zen_s ID_0\tau_s}{15\varepsilon r\omega RB_p}. \qquad (6.26)$$

This counter-current is also small, but could become interesting near the pedestal for $\omega\tau_s v_{\text{quiv}}^2 \sim \varepsilon v_0^2 \gg \varepsilon v_i^2$.

https://doi.org/10.1017/S0022377818001071 Published online by Cambridge University Press

Symmetric spectrum current will be driven in the deuterium as well as the alphas, however, because its charge number is the same as that of tritium it results in no net parallel driven current according to (1.7). Interestingly, comparing (5.31) with (6.23), suggests that the ratio of alpha over deuterium driven currents might approach order unity

$$\frac{J_{\rm alpha}}{J_D} \simeq \frac{2\pi^{1/2} n_s v_c^3}{9 n_D v_D^3} \sim \frac{v_c^3}{v_D v_0^2}, \tag{6.27}$$

for $1 \gg n_s/n_D \gtrsim v_D^2/v_0^2$. This estimate also suggests that the alpha current is significant.

For symmetric spectrum current driven alphas we assume the heated species is predominately deuterium. The flux surface averaged minority heating power absorbed by the nearly Maxwellian deuterium is evaluated as in § 5 to obtain

$$P_D \simeq \frac{n_D M_D v_{\rm quiv}^2 \omega}{\pi \varepsilon}, \tag{6.28}$$

for on axis heating with $(qv/\varepsilon r\omega)^2 \ll 1$. Even though the minority heating power absorbed by the alphas is roughly $n_s M/n_D M_D \ll 1$ smaller, (6.27) implies that it may be possible to drive significant symmetric spectrum alpha current.

In summary, (6.23) seems to give the most useful measure of the symmetric spectrum alpha current being driven when the applied power predominately goes into heating the deuterium minority.

7. Summary

The preceding sections have tried to provide insight into the treatment of effects associated with finite radial drift departures from flux surfaces. The distinction between flux and drift surfaces becomes significant whenever the poloidal gyroradius approaches radial scale lengths of interest. Section 3 demonstrates the appearance of what seem like 'radial' derivatives, but are actually derivatives with respect to canonical angular momentum, when velocity and configuration space variables are mixed (as when action-angle variables are employed). When the current and charge density for full wave treatments is evaluated using these descriptions they must be consistent with a quasilinear operator that conserves particles as noted in § 2.

In § 4 the QL operator of Catto *et al.* (2017) is transit averaged over the full streaming operator including drifts as well as parallel streaming. This extension of the transit average allows the distinction between flux and drift surfaces to be retained since the transit average now follows a drifting particle rather than assuming the charge moves on a flux surface.

The generalized transit average allows finite poloidal gyroradius effects on minority heating to be evaluated in § 5 for minority heating. There it is shown that it is possible to drive a small minority counter-current with a symmetric spectrum for near Maxwellian minority species as a secondary effect. As much higher levels of heating are normally employed to obtain strong non-Maxwellian minority features it is possible that larger, desirable amounts of symmetric spectrum net co-current can be driven without any additional power input and that it might compete with the bootstrap current. Simulations will be needed to determine whether this is actually possible.

Symmetric spectrum driven alpha counter-current can also arise from minority heating of deuterium in a tritium plasma without added power input. The evaluation

https://doi.org/10.1017/S0022377818001071 Published online by Cambridge University Press

of this current in § 6 indicates it might be possible to drive an overall net co-current at very high heating levels, even though the energetic alpha density is much lower than the background plasma density. The driven alpha and deuterium currents seem comparable, but unlike the alphas, the deuterium current does not result in a net parallel current.

An estimate of a related finite counter-current driven by the asymmetry of the electron drag on the alphas (Cottrell & Start 1991) indicates that it might also become of interest at very high heating levels where it might conceivably compete with the bootstrap current.

To drive symmetric spectrum current in the co-current direction requires heating $v_{||} < 0$ ($v_{||} > 0$) minorities or alphas more than those with $v_{||} > 0$ ($v_{||} < 0$) for $I = RB_t > 0$ ($I < 0$). The examples given here drive minority counter-current with a symmetric spectrum, and thereby yield net co-current. The results presented assumed slow spatial variation of $|\boldsymbol{e}_m \cdot [\boldsymbol{n} v_{||} J_p(w) + \boldsymbol{e}_{\perp p} v_\perp]|^2$ in (4.13), (4.14) and (4.17), and assumed $|\boldsymbol{e}_m \cdot \boldsymbol{e}_+|^2 \simeq |\boldsymbol{e}_m \cdot \boldsymbol{e}_+|^2_*$ in (5.2). Another possibility is to retain the minority heating profile variation on a near poloidal gyroradius scale by Taylor expansion

$$\begin{aligned} |\boldsymbol{e}_m \cdot \boldsymbol{e}_+|^2 &\simeq |\boldsymbol{e}_m \cdot \boldsymbol{e}_+|^2_* + (\psi - \bar{\psi}_*)\partial |\boldsymbol{e}_m \cdot \boldsymbol{e}_+|^2/\partial\psi + \cdots \\ &= |\boldsymbol{e}_m \cdot \boldsymbol{e}_+|^2_* + (I v_{||}/\Omega)\partial |\boldsymbol{e}_m \cdot \boldsymbol{e}_+|^2/\partial\psi + \cdots . \end{aligned} \tag{7.1}$$

Then it may be possible to focus the rf in such a way that at the resonant layer

$$|\boldsymbol{e}_m \cdot \boldsymbol{e}_+|^{-2}\partial |\boldsymbol{e}_m \cdot \boldsymbol{e}_+|^2/\partial\psi < 0. \tag{7.2}$$

This capability would drive minority counter-current, and our minority result (5.31) would become

$$J^{\rm rf}_{\rm min} \simeq \frac{12 Z e n_m v_m^3 \tau_s I}{5\pi^{1/2}\varepsilon(4v_c^3 + v_\lambda^3)} \frac{\partial v^2_{\rm quiv}}{\partial\psi}, \tag{7.3}$$

while our alpha result (6.23) would become

$$J^{\rm rf}_{\rm alpha} \simeq \frac{Z e n_s I \tau_s}{15\varepsilon} \frac{\partial v^2_{\rm quiv}}{\partial\psi}, \tag{7.4}$$

since we need only make the substitution

$$I v_{||}/RB_p r\Omega \to -(I v_{||}/\Omega |\boldsymbol{e}_m \cdot \boldsymbol{e}_+|^2)\partial |\boldsymbol{e}_m \cdot \boldsymbol{e}_+|^2/\partial\psi . \tag{7.5}$$

It seems unlikely that precise control of the minority heating profile is practical, but nonetheless strong variation of the applied rf electric field can occur and it may be possible to detect these co and counter driven currents in simulations of symmetric spectrum minority heating at high rf levels of $\omega\tau_s v^2_{\rm quiv} \gg \varepsilon v_i^2$. The estimates in this section and the preceding sections are at best indicative of actual driven currents.

Acknowledgements

Work supported by the US Department of Energy grant DE-FG02-91ER-54109 at MIT. I am grateful to A. Ram for several suggestions that improved the presentation.

REFERENCES

ANTONSEN, T. M. JR. & CHU, K. R. 1982 Radio frequency current generation by waves in toroidal geometry. *Phys. Fluids* **25**, 1295–1296.

BRAMBILLA, M. 1999 Numerical simulation of ion cyclotron waves in tokamak plasmas. *Plasma Phys. Control. Fusion* **41**, 1–34.

https://doi.org/10.1017/S0022377818001071 Published online by Cambridge University Press

CALVO, I. & PARRA, F. I. 2012 Long-wavelength limit of gyrokinetics in a turbulent tokamak and its intrinsic ambipolarity. *Plasma Phys. Control. Fusion* **54**, 115007.

CATTO, P. J. 1978 Linearized gyrokinetics. *Plasma Phys.* **20**, 719–722.

CATTO, P. J., LEE, J.-P. & RAM, A. K. 2017 A quasilinear operator retaining magnetic drift effects in tokamak geometry. *J. Plasma Phys.* **83**, 905830611.

CATTO, P. J. & MYRA, J. R. 1992 A quasilinear description for fast wave minority heating permitting off magnetic axis heating in a tokamak. *Phys. Fluids* B **4**, 187–199.

CATTO, P. J., MYRA, J. R. & RUSSELL, D. A. 1994 A quasilinear, Fokker–Planck description of fast wave minority heating permitting off-axis tangency interactions. *Phys. Plasmas* **1**, 52–63.

CATTO, P. J., TANG, W. M. & BALDWIN, D. E. 1981 Generalized gyrokinetics. *Plasma Phys.* **23**, 639–650.

CHAPMAN, I. T., GRAVES, J. P., LENNHOLM, M., FAUSTIN, J., LERCHE, E., JOHNSON, T. & THOLERUS, S. 2015 The merits of ion cyclotron resonance heating schemes for sawtooth control in tokamak plasmas. *J. Plasma Phys.* **81**, 365810601.

COTTRELL, G. A. & START, D. F. H. 1991 A large-orbit model of fast ion slowing down during ICRH: comparison with JET data. *Nucl. Fusion* **31**, 61–71.

ERIKSSON, L.-G. & HELANDER, P. 1994 Monte Carlo operators for orbit-averaged Fokker–Planck equations. *Phys. Plasmas* **1**, 308–314.

ERIKSSON, L.-G., MANTSINEN, M., BORBA, D., FASOLI, A., HEETER, R., SHARAPOV, S., START, D. F. H., CARLSSON, J., GONDHALEKAR, A., HELLSTEN, T. *et al.* 1998 Evidence for a wave-induced particle pinch in the presence of toroidally asymmetric ICRF waves. *Phys. Rev. Lett.* **81**, 1231–1234.

FISCH, N. J. 1981 Current generation by minority-species heating. *Nucl. Fusion* **21**, 15–22.

HELANDER, P. & CATTO, P. J. 2001 Neoclassical current drive by waves with a symmetric spectrum. *Phys. Plasmas* **8**, 1988–1994.

HELLSTEN, T., CARLSSON, J. & ERIKSSON, L.-G. 1995 Minority ion cyclotron current drive in tokamaks. *Phys. Rev. Lett.* **74**, 3612–3615.

JAEGER, E. F., BERRY, L. A., DAZEVEDO, E., BATCHELOR, D. B., CARTER, M. D. & WHITE, K. F. 2002 Advances in full-wave modeling of radio frequency heated, multidimensional plasmas. *Phys. Plasmas* **9**, 1873–1881.

KAGAN, G. & CATTO, P. J. 2008 Arbitrary poloidal gyroradius effects in tokamak pedestals and transport barriers. *Plasma Phys. Control. Fusion* **50**, 085010-25.

KAUFMAN, A. N. 1972 Quasilinear diffusion of an axisymmetric toroidal plasma. *Phys. Fluids* **15**, 1063–1069.

KENNEL, C. F. & ENGELMANN, F. 1966 Velocity space diffusion from weak plasma turbulence in a magnetic field. *Phys. Fluids* **9**, 2377–2388.

LEE, X. S., MYRA, J. R. & CATTO, P. J. 1983 General frequency gyrokinetics. *Phys. Fluids* **26**, 223–229.

MANTSINEN, M. J., INGESSON, L. C., JOHNSON, T., KIPTILY, V. G., MAYORAL, M.-L., SHARAPOV, S., ALPER, B., BERTALOT, L., CONROY, S., ERIKSSON, L.-G. *et al.* 2002 Controlling the profile of ion-cyclotron-resonant ions in JET with the wave-induced pinch effect. *Phys. Rev. Lett.* **89**, 115004-4.

PARRA, F. I. & CALVO, I. 2011 Phase-space Lagrangian derivation of electrostatic gyrokinetics in general geometry. *Plasma Phys. Control. Fusion* **53**, 045001.

PARRA, F. I. & CATTO, P. J. 2008 Limitations of gyrokinetics on transport time scales. *Plasma Phys. Control. Fusion* **50**, 065014.

PARRA, F. I. & CATTO, P. J. 2010 Transport of momentum in full f gyrokinetics. *Phys. Plasmas* **17**, 056106.

PETROV, YU. V. & HARVEY, R. W. 2016 A fully-neoclassical finite-orbit-width version of the CQL3D Fokker–Planck code. *Plasma Phys. Control. Fusion* **58**, 115001.

STIX, T. H. 1975 Fast-wave heating of a two-component plasma. *Nucl. Fusion* **15**, 737–754.

https://doi.org/10.1017/S0022377818001071 Published online by Cambridge University Press